Available online at www.sciencedirect.com
ScienceDirect
Geochimica et Cosmochimica Acta 70 (2006) 4491–4506
Geochimica
www.elsevier.com/locate/gca

Chemical characteristics of dissolved organic nitrogen in an oligotrophic subtropical coastal ecosystem

Nagamitsu Maie [a], Kathleen J. Parish [a], Akira Watanabe [b], Heike Knicker [c], Ronald Benner [d], Tomonori Abe [b], Karl Kaiser [d], Rudolf Jaffé [a,*]

[a] Southeast Environmental Research Center, and Department of Chemistry and Biochemistry, Florida International University, Miami, FL 33199, USA
[b] Department of Cycling Resources, School of Bioagricultural Sciences, Nagoya University, Chikusa, Nagoya 464-8601, Japan
[c] Lehrstuhl für Bodenkunde, Technische Universität München, 85350 Freising, Weihenstephan, Germany
[d] Department of Biological Sciences and Marine Science Program, University of South Carolina, Columbia, SC 29208, USA

Received 1 February 2006; accepted in revised form 23 June 2006

Abstract

Water samples were collected from rivers and estuarine environments within the Florida Coastal Everglades (FCE) ecosystem, USA, and ultrafiltered dissolved organic matter (UDOM; <0.7 μm, >1 kDa) was isolated for characterization of its source, bioavailability and diagenetic state. A combination of techniques, including ^{15}N cross-polarization magic angle spinning nuclear magnetic resonance (^{15}N CPMAS NMR) and X-ray photoelectron spectroscopy (XPS), were used to analyze the N components of UDOM. The concentrations and compositions of total hydrolysable amino acids (HAAs) were analyzed to estimate UDOM bioavailability and diagenetic state. Optical properties (UV–visible and fluorescence) and the stable isotope ratios of C and N were measured to assess the source and dynamics of UDOM. Spectroscopic analyses consistently showed that the major N species of UDOM are in amide form, but significant contributions of aromatic-N were also observed. XPS showed a very high pyridinic-N concentration in the FCE–UDOM (21.7 ± 2.7%) compared with those in other environments. The sources of this aromatic-N are unclear, but could include soot and charred materials from wild fires. Relatively high total HAA concentrations (4 ± 2% UDOC or 27 ± 4% UDON) are indicative of bioavailable components, and HAA compositions suggest FCE–UDOM has not undergone extensive diagenetic processing. These observations can be attributed to the low microbial activity and a continuous supply of fresh UDOM in this oligotrophic ecosystem. Marsh plants appear to be the dominant source of UDOM in freshwater regions of the FCE, whereas seagrasses and algae are the dominant sources of UDOM in Florida Bay. This study demonstrates the utility of a multi-technique and multi-proxy approach to advance our understanding of DON biogeochemistry.

1. Introduction

Dissolved organic matter (DOM) is the major form of organic matter (OM) in most aquatic environments (Findlay and Sinsabaugh, 2003) and this is especially true for oligotrophic ecosystems where the contribution of suspended particles is quite low (Wangersky, 1993). DOM influences the physicochemical characteristics of natural aquatic systems by increasing light attenuation, maintaining pH through organic acid buffering, acting as a strong ligand for many elements, and affecting the heat balance and the redox chemistry of trace metals (Aitkenhead-Peterson et al., 2003). Furthermore, DOM is known to fuel the microbial loop.

As for microbial loop energetics, dissolved organic nitrogen (DON) is very important especially in oligotrophic environments where most of the nitrogen (N) is in the dissolved organic form (Boyer et al., 1997; Bronk, 2002). A significant portion of DON may be remineralized by microbes depending upon ambient nutrient status, C:N:P ratio of source materials (Tezuka, 1990), and the chemical stability and bioavailability of DOM (Benner et al., 1986; Amon and Benner, 1996).

* Corresponding author. Fax: +1 305 348 4096.
E-mail address: jaffer@fiu.edu (R. Jaffé).

0016-7037/$ - see front matter © 2006 Elsevier Inc. All rights reserved.
doi:10.1016/j.gca.2006.06.1554

The Florida Coastal Everglades (FCE) is an oligotrophic, subtropical wetland located in the southern part of the Florida Peninsula, USA. There, most nutrient biogeochemistry studies to date have focused on dissolved inorganic nutrients (N and P), as these fractions are directly available for phytoplankton uptake (Tomas et al., 1998; Brand, 1999). However, DON is often the major form of N in aquatic ecosystems (Wangersky, 1993; Boyer et al., 1997; Davis et al., 2001; Bronk, 2002) and therefore represents a potential source of N to phytoplankton and bacteria (Carlsson and Graneli, 1993).

Continuous population growth in southern Florida is ever increasing the demand for water, thus securing adequate water resources is a pressing challenge. Anthropogenic activities have caused decreased freshwater inputs from the Everglades into Florida Bay (FB) (Robblee et al., 1991), which are blamed for the recent rapid decline in the health of FB, evident by seagrass die-off and increased algal blooms (Zieman et al., 1999). Public awareness of the degrading health of FB has been an important impetus for one of the largest natural restoration projects designed to return a more natural flow regime to the Everglades ecosystem (http://www.evergladesplan.org/). However, hydrological changes might bring about adverse effects in the Everglades ecosystem by increasing nutrient inputs. While the Everglades ecosystem is largely P limited (Fourqurean et al., 1993; Phlips and Badylak, 1996; Boyer et al., 1997; Lavrentyev et al., 1998), there is evidence that the system does respond to N inputs (Lavrentyev et al., 1998; Brand, 1999). For example, algal blooms in FB are sometimes stimulated by N enrichment (Boyer and Keller, 2003) and work by Childers and Wozniak (pers. comm.) on ^{15}N isotope data indicate substantial N uptake adjacent to canals. However, little is known about the composition, sources and bioavailability of DON in this system.

The main objective of this study was the molecular characterization of the ultrafiltered high molecular weight (HMW) fraction (>1000 Da) of DON (UDON). UDON is a significant component of the DON pool (Benner et al., 1992; Aluwihare et al., 2005), as such it may play an important role in the Everglades N cycle. Many DON bioavailability studies have focused on low molecular weight (LMW) DON components (Wheeler and Kirchman, 1986; Palenik and Morel, 1990; Keil and Kirchman, 1991) while a major portion of DON presumably consists of HMW compounds (Thurman, 1985; Seitzinger and Sanders, 1997; Aluwihare et al., 2005). Not much is known about the bioavailability of UDON, but recent data indicate that it may be an important source of N for bacteria (Amon and Benner, 1994, 1996) and picoplankton (Berg et al., 2003). Larger molecules, once thought to be mainly refractory, have also been shown to release N-rich, biologically available compounds upon exposure to sunlight (Bushaw et al., 1996; Obernosterer and Benner, 2004). Determining the chemical speciation and assessing the potential bioavailability of UDON are crucial steps in understanding the importance of DON to microorganisms (Bronk and Gilbert, 1993; Feuerstein et al., 1997; Aluwihare et al., 2005) and its potential influence on coastal eutrophication. Most coastal eutrophication studies have been performed at temperate latitudes (Cloern, 2001), although the source and biogeochemical processing of nutrients are considered to be different across different climatic zones. This work will encompass a fresh water to marine transect in a subtropical, oligotrophic coastal wetland ecosystem, namely the FCE.

In order to investigate the source and characteristics of UDOM, we measured optical properties (UV and fluorescence) and C and N stable isotope ratios. ^{15}N cross-polarization magic angle spinning nuclear magnetic resonance (^{15}N CPMAS NMR) spectroscopy and X-ray photoelectron spectroscopy (XPS) were used to identify different N species. Acid-hydrolysable amino acids (HAAs) were also analyzed because they have been shown to be a dominant (Vairavamurthy and Wang, 2002) and bioavailable DON form (Palenik and Morel, 1990; Simon and Rosenstock, 1992; Kroer et al., 1994), as such they could provide valuable information concerning its bioavailability, degree of degradation and overall environmental dynamics.

2. Materials and methods

2.1. Study area

The Everglades is located at the southern tip of the Florida peninsula, USA, and supplies freshwater to the Gulf of Mexico and to FB (Fig. 1). The Everglades ecosystem is P deficient (total P concentration of freshwater sites is typically <0.25 μmol L^{-1}), and is dependent on dry and wet deposition for nutrient inputs (Davis, 1994; Childers et al., 2006), contrasting with other wetlands that receive most of their nutrients via river inputs.

This work focuses on five distinct study sites ranging from freshwater, estuarine, to marine ecosystems along the two major drainage paths through the Everglades

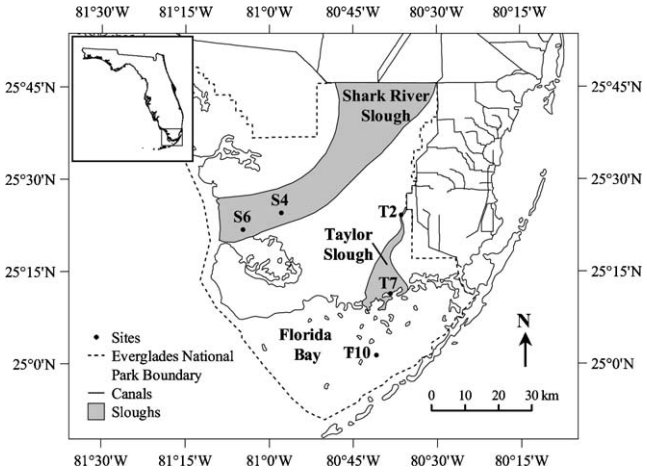

Fig. 1. Location of sampling sites.

(Fig. 1). Two sites, designated as S4 and S6, are located along Shark River Slough (SRS). Two other sites (T2 and T7) are located along Taylor Slough (TS). The fifth site (T10) is centrally located in FB.

Shark River Slough is a broad shallow waterway and its freshwater marshes are covered mainly by sawgrass (*Cladium jamaicense*) with interspersed spike rush (*Eleocharis* sp.), thick benthic periphyton mats, and tree islands (Davis, 1994). The vegetation at S4 and S6 is mainly dominated by red mangroves (*Rhizophora mangle*). The plant community in TS is similar to SRS but the water is shallower and the hydroperiods are shorter. Site T2 is located in a sawgrass/spikerush/periphyton dominated freshwater wetland. Site T7 is located at the mouth of the Taylor River in an area dominated by fringe mangrove forests with seasonally driven freshwater inputs and wind driven estuarine inputs. The soil type along the SRS and TS transects are a peat and marl, respectively. In contrast, FB is a large (2000 km^2), shallow, semi-enclosed, micro-tidal estuarine system, where the main vegetation is seagrass, mainly turtle grass, *Thalassia testudinum* (Zieman et al., 1989). More detailed information on these sampling sites can be found elsewhere (Childers et al., 2006).

2.2. Sample collection and processing

Surface water samples were collected in 25-L low density polyethylene bottles during the early part of the dry season (from Dec 2001 to Jan 2002). The bottles were cleaned by soaking them with 0.5 mol L^{-1} HCl followed by 0.1 mol L^{-1} NaOH for 24 h each. Water samples were filtered through pre-combusted (470 °C for 4 h) GF/F glass fiber filters (nominal pore size, 0.7 μm; Whatman International Ltd., Maidstone, England) and concentrated using a Pellicon 2 Mini tangential flow ultrafiltration system equipped with a nominal 1 kDa molecular weight cut-off regenerated cellulose membrane (Millipore Co., Billerica, MA, USA) (Maie et al., 2005). During ultrafiltration the samples were cooled in ice water. In the case of the saline water sample (T10), the salts were eliminated by diafiltration with one liter of Milli-Q water (Millipore) to the concentrated sample and then re-concentrated to 100 mL. This was repeated three times. Subsequently, the concentrated samples were freeze-dried and powdered with an agate mortar and pestle for further analysis. Ancillary data for the whole water samples are listed below in the order of sites S4, S6, T2, T7, and T10: DOC, 1.22, 1.18, 0.74, 0.93, and 0.69 mmol L^{-1}; TN, 40, 46, 32, 55, and 34 μmol L^{-1}; TON, 37, 44, 30, 47, and 33 μmol L^{-1}; TP, 0.16, 0.43, 0.12, 0.58, and 0.11 μmol L^{-1} (see Childers et al., 2006; for the analytical method).

2.3. Optical measurements

For the fluorescence and UV–Vis absorption spectra, UDOM solutions of approximately 5 mgC L^{-1} (20 mgC L^{-1} for T10) were prepared in a 0.05 M tris(hydroxymethyl)aminomethane (THAM) buffer solution, which was adjusted to pH 7.0 with phosphoric acid. After dissolution, all UDOM solutions were filtered through precombusted (470 °C for 4 h) GF/F filters.

The UV–Vis absorption spectra were measured with a Shimadzu UV-2102PC spectrophotometer between 250 and 800 nm in a 1 cm quartz cuvette. Two optical parameters were determined: (1) the specific UV absorbance at 254 nm ($SUVA_{254}$) and (2) the UV spectral slope (S). The $SUVA_{254}$ parameter is defined as the UV absorbance at 254 nm measured in inverse meters (m^{-1}) divided by the DOC concentration (mg L^{-1}) (Weishaar et al., 2003). The S parameter is obtained by fitting the absorption data to a simple exponential equation (Blough and Green, 1995). The S parameter is known to be sensitive to baseline offsets; therefore, to correct for this, the average absorbance from 700 to 800 nm was subtracted from each spectrum (Green and Blough, 1994).

Fluorescence spectra were measured with a Jobin–Yvon–Horiba (France) Spex Fluoromax-3 fluorometer equipped with a 150-W continuous output xenon arc lamp. Two single emission fluorescence scans were obtained at excitation wavelengths of 313 nm and 370 nm. For each scan, fluorescence intensity was recorded at emission wavelengths ranging from 330 to 500 nm and from 385 to 550 nm, respectively. The bandpass was set at 5 nm for excitation and emission wavelengths. From the 313 nm scan the maximum emission intensity (F_{max}) and maximum emission wavelength (λ_{max}) were determined (Donard et al., 1989; Sierra et al., 1994, 1997). From the 370 nm scan a fluorescence index (FI) was calculated (McKnight et al., 2001). Originally, the fluorescence index was introduced as a ratio of emission intensities at 450 and 500 nm at an excitation wavelength of 370 nm (McKnight et al., 2001). However, we noticed that after fully correcting fluorescence intensity values (including instrument bias corrections) there was a shift of emission maximum to longer wavelengths. Thus, we modified the fluorescence index and used the ratio of fluorescence intensities at 470 and 520 nm, instead of 450 and 500 nm. Similar modifications are being considered by McKnight and co-workers (Cory, 2006). Since comparison of FI values among published data was difficult due to inconsistent spectrum corrections in the literature, in this study, interpretation was conducted based on the comparison within our sample set only.

For excitation–emission matrix (EEM) measurements, forty emission scans were acquired at excitation wavelengths (λ_{ex}) between 260 and 455 nm at 5 nm intervals. The emission wavelengths were scanned from $\lambda_{ex} + 10$ nm to $\lambda_{ex} + 250$ nm at 2 nm intervals (Coble et al., 1993; Coble, 1996). The individual spectra were concatenated to form a three-dimensional excitation–emission matrix (EEM). Data was processed using Excel (version 11 Microsoft) and SigmaPlot (version 7 SPSS Inc.).

All fluorescence spectra were acquired in ratio mode whereby the sample (emission signal, S) and reference (excitation lamp output, R) signals were collected and the ratio (S/R) was calculated. The ratio mode eliminates the

influence of possible fluctuation and wavelength dependency of excitation lamp output. Several post-acquisition steps were involved in the correction of the fluorescence spectra. First, an inner filter correction was applied to the fluorescence data according to McKnight et al. (2001). After inner filter corrections, the sample EEM underwent spectral subtraction of the buffer solution to remove most of the effects due to Raman scattering. Instrument bias related to wavelength dependent efficiencies of the specific instrument's optical components (gratings, mirrors, etc) were then corrected by applying multiplication factors, supplied by the manufacturer, for both excitation and emission wavelengths for the range of observations. Finally, the fluorescence intensity values were converted to quinine sulfate unit (QSU) to facilitate inter-laboratory comparisons (Coble et al., 1993).

2.4. Analyses of C and N concentrations and stable isotope ratios

Carbonates in UDOM samples were removed prior to analyses using acid vapor decarbonation (Hedges et al., 1994). Briefly, samples were weighed in duplicate (ca. 2–5 mg) into silver capsules (8× 5 mm, Elemental Microanalysis Ltd.) and exposed to hydrochloric acid vapor for 4 h. Acid vapor was removed under vacuum until there was no noticeable acid smell. Analytical artifacts due to decarbonation on the concentration and stable isotope ratio measurements for N are reported to be negligible (Lorrain et al., 2003). Organic C and total N concentrations were measured using a Carlo Erba NA 1500 Nitrogen/Carbon Analyzer (Carlo Erba, Milan, Italy). C and N stable isotopic analyses were measured on a ThermoFinnigan Delta C isotope ratio mass spectrometer. Isotopic ratios are reported in the standard delta notation: δ value (‰) = $[(R_{sample}/R_{standard}) - 1] \times 1000$. Results are presented with respect to the international standards of atmospheric N (AIR N_2) and Vienna Pee Dee belemnite (V-PDB) for C. Duplicate measurements were conducted and reproducibility was ±1.5‰ for $\delta^{15}N$ and ±0.2‰ for $\delta^{13}C$ on average.

2.5. ^{15}N CPMAS-NMR

^{15}N CPMAS-NMR spectra were obtained on a Bruker DMX 400 (40.56 MHz) spectrometer (Bruker BioSpin GmbH, Rheinstetten, Germany) using a ramped pulse sequence (Peersen et al., 1993; Cook et al., 1996), a rotation frequency of 4.4 kHz, a contact time of 1 ms, and a pulse delay of 200 ms. Previous studies (Knicker and Lüdemann, 1995) revealed that for humic materials, this pulse delay should be long enough to avoid saturation. Between 6.4×10^5 and 1.3×10^6 single scans were accumulated and line broadenings of 50–150 Hz were applied. The chemical shift was referenced to nitromethane scale (=0 ppm) and was adjusted with ^{15}N-enriched glycine (−347.6 ppm). The quantification of each N species was not conducted due to low signal-to-noise ratio of ^{15}N NMR spectra.

2.6. XPS-N1s spectra

XPS-N1s spectra were recorded on an X-ray photoelectron spectrometer (ESCA-3300, Shimadzu) using Mg Kα non-monochromatic radiation with an analyzer pass energy of 32 eV, an electric current of 30 mA, and a voltage of 10 kV. A detailed description on this method can be found in Abe and Watanabe (2004). Briefly, a finely powdered sample (ca. 1 mg) was fixed on the surface of a metallic sample block by means of Scotch® double-sided nonconducting tape (3 M, Saint Paul, MI, USA). Spectra were recorded for each visible line with 0.05 eV per step. The time for one scan was set at 298 ms, and between 126–160 scanned data were accumulated. Correction of binding energy was made relative to the C–C/C–H signal at 385.0 eV in the C1s spectra measured simultaneously. The spectra were deconvoluted into three major N species depending on its binding energy (solid lines), by applying three Gaussian curves with peak centers at 399.0 ± 0.1 eV (pyridinic N including imine, pyridine, aromatic amine, and NH in guanidine), 400.4 ± 0.1 eV (peptide bond N including other amides, pyrrole, secondary and tertiary amines, and imide), and 402.3 ± 0.1 eV (primary amine N including protonated amine; Abe and Watanabe, 2004). The proportions of the three N groups were estimated from the relative spectral areas surrounded by Gaussian curves and the base line. The detection limit and the reproducibility of this measurement are ca. 1.5 atomic% and <1 atomic%, respectively (Abe and Watanabe, 2004).

2.7. Amino acid analysis

Amino acid analysis was performed according to Hedges et al. (1994). Greater detail can be found in Cowie and Hedges (1992). Amino acids were separated on a Licrospher 100 RP18 HPLC column (250 mm × 4 mm, 5 μm) with a guard column (5 mm × 4 mm) after in-line derivatisation with OPA/mercaptoethanol at 30 °C. The system was an Agilent HP 1100 system with an auto sampler and fluorescence detector controlled by HP Chemstation software. Powdered UDOM samples were hydrolyzed in 6 M HCl in the presence of ascorbic acid at 110 °C for 20 h and processed for HPLC analysis according to Kaiser and Benner (2005). A total of 10 μl of the processed sample was mixed inline with 10 μl of 0.5 M borate acid buffer (pH 9.5) and 10 μl OPA/mercaptoethanol reagent.

Method program and gradient were as follows: Solvent A was 29 mM sodium acetate adjusted to pH 6.2. Solvent B was methanol. Amino acid derivatives were separated with a linear binary gradient starting with 77% A to 71% A at 4 min, then 56% A at 20 min and 20% A at 33 min. After 33 min the system was retuned to 77% A and equilibrated for 3 min. The flow rate was 0.9 ml min^{-1}, and total run time was 36 min. Excitation was at 350 nm and emission of OPA derivatives was recorded at 420 nm. A total of 19 individual AAs were analyzed, 15 of which were protein AAs (aspartic acid, Asp; glutamic acid, Glu; serine, Ser;

histidine, His; glycine, Gly; threonine, Thr; arginine, Arg; alanine, Ala; tyrosine, Tyr; methionine, Met; valine, Val; phenylalanine; Phe; isoleucine, Ile; leucine, Leu; lysine, Lys) and four non-protein AAs (β-alanine (BALA), γ-aminobutyric acid (GABA), α-aminobutyric acid (AABA), and ornithine (Orn)).

A degradation index (DI), which was introduced to evaluate the diagenetic state of particulate OM (POM) by using HAA composition (Dauwe et al., 1999), was calculated for our UDOM samples. The concept of DI is that when natural OM (NOM) samples with different diagenetic histories are subjected to principal component analysis (PCA) based on their AA composition (mol%), the first principal component (PC1) represents the degree of diagenesis, therefore the score plot of PC1 is referred to as DI. The DI values can be compared among researchers by quoting reference dataset (average, SD, and factor coefficient) in the literature to the following equation:

$$\mathrm{DI} = \sum_i \left[\frac{\mathrm{var}_i - \mathrm{AVEvar}_i}{\mathrm{SDvar}_i}\right] \times \mathrm{fac}\cdot\mathrm{coef}_i$$

where var_i is the mol% of AA i in a sample to be examined, and AVEvar_i, SDvar_i, and $\mathrm{fac}\cdot\mathrm{coef}_i$ are average, standard deviation (SD), and factor coefficient of AA i of reference dataset, respectively (Dauwe et al., 1999). The DI was calculated by using two reference datasets; one ($\mathrm{DI_D}$) was calculated referring the HAA composition of DOM to that from estuarine to open ocean environments (Yamashita and Tanoue, 2003a), and another ($\mathrm{DI_P}$) was that of POM collected from a variety of marine environments (Dauwe et al., 1999). Amino acid composition (mol%) was re-calculated to fit their dataset beforehand. Since tryptophan (Trp) was not measured in our experiment, the Trp concentration was taken to be 0 in this calculation.

3. Results and discussion

3.1. Optical and chemical characteristics of FCE–UDOM

3.1.1. UV–visible absorption spectroscopy

The $\mathrm{SUVA_{254}}$ parameter, which tracks chromophoric DOM (CDOM) concentrations, has been used as a proxy for the aromaticity of DOC (Traina et al., 1990; Weishaar et al., 2003) or to assess the relative abundance of the humic fraction (Dilling and Kaiser, 2002). The $\mathrm{SUVA_{254}}$ was the highest at the mangrove sites (T7, S4, and S6; 8.1 ± 0.5), quite low at the FB site (0.86), and intermediate at the T2 freshwater marsh site (4.2) (Table 1). The S value is a measure of how rapidly absorption decreases as the wavelength increases (Blough and Green, 1995). This parameter has been used to describe different types and sources of CDOM (Blough and Green, 1995; McKnight et al., 1997; Battin, 1998). The S values for the three mangrove sites are all very similar (0.0137 ± 0.0002) and fall in the range typical of coastal brown waters (0.011–0.018, more typical values 0.014–0.016 for river end members) (Blough and Vecchio, 2002). The remaining two sites (T2 and T10) exhibit higher S values (~0.016) but still lower than those of off-shore and open ocean waters, ~0.025 (Blough and Vecchio, 2002), suggesting a mixed microbial-terrestrial UDOM source.

3.1.2. Fluorescence spectroscopy

3.1.2.1. Single emission scan measurements. Two single scan fluorescence indices, λ_{max} and FI, have been used as a quick, simple means of distinguishing the sources of CDOM in the FCE (Lu et al., 2003; Jaffé et al., 2004; Maie et al., 2006a). DOM with terrestrial/higher plant origin typically has lower FI values and longer maximum wavelength (λ_{max}) than that with marine/microbial origin (Donard et al., 1989; Sierra et al., 1994; McKnight et al., 2001). The fluorescence spectroscopic properties of our samples are presented in Table 1. The fluorescence index (FI) ranged from 1.10 to 1.35 with lower values from mangrove site UDOM samples (T7, S4, and S6; 1.11 ± 0.02) with an intermediate value for the freshwater marsh site T2 (1.25) and the highest value at FB site T10 (1.35). The λ_{max} ranged from 468 to 480 nm with a shorter value from T10, intermediate value for freshwater marsh site, and longer values for the mangrove sites. The FI and λ_{max} values of UDOM samples were low and long, respectively, compared with those of whole water samples (Maie and Jaffé, unpublished data), suggesting that the more conjugated aromatic moiety of DOM (McKnight et al., 2001) was preferentially concentrated in the UDOM fraction.

3.1.2.2. EEM spectroscopy. Fluorescence EEM spectroscopy is a tool that can potentially provide complete spectral characterization of CDOM and is used to differentiate classes of fluorophores (e.g., Kowalczuk et al., 2003; Stedmon et al., 2003). The contour plots show two main types of EEM spectra for the FCE–UDOM samples. The freshwa-

Table 1
UV–visible optical parameters and fluorescence emission scans at 313 and 370 nm excitation wavelength

Sample site	UV–visible		370 nm Excitation		313 nm Excitation	
	$\mathrm{SUVA_{254}}$ ($\mathrm{m^{-1}}$)	S-value ($\times 10^3$ $\mathrm{nm^{-1}}$)	F_{max} (QSU)	FI f_{470}/f_{520}	λ_{max} (nm)	F_{max} (QSU)
T2	4.2	16.1	65	1.25	450	111
T7	7.6	13.8	50	1.13	458	79
T10	0.86	15.9	7.8	1.35	408	20
S4	8.1	13.9	78	1.11	458	129
S6	8.5	13.5	63	1.10	461	101

ter/coastal sites (T2, T7, S4, and S6) are very similar in appearance and characteristic of terrestrially derived DOM with strong terrestrial humic signals (peaks A and C; Fig. 2a). The FB site (T10) is more marine-like with predominance of marine humic-like (peak M) and protein-like fluorescence (peaks B and T) (Fig. 2b). This difference in the UDOM characteristics indicates a change in the source and/or processing between the freshwater/mangrove sites and the FB estuary.

Peak A has the similar excitation wavelength as peak C but the blue-shift in the emission of peak A indicates the fluorophore has less aromaticity or fewer functional groups (less conjugated electron resonance system) than that responsible for peak C (Coble et al., 1998). Thus, the ratio of peak intensities (A:C) can give information on the composition and also diagenetic state of the CDOM. The ratios for the freshwater/coastal UDOM samples are all similar with values of 2.6 ± 0.2 (Table 2). These values are on the higher side compared to those from a variety of waters (Coble, 1996), and suggest the FCE–UDOM being less degraded/reworked or having undergone a significant amount of photodegradation (Coble, 1996).

Protein-like fluorescence is attributed to the aromatic AAs in the UDOM samples. Two fluorescent protein peaks, a Tyr-like peak (B) and a Trp-like peak (T), have been identified in DOM samples (e.g., Coble, 1996; Yamashita and Tanoue, 2003b). Such protein-like fluorescence was small in all UDOM samples except for T10, making it difficult to locate exact peak maxima. Furthermore, other fluorophore(s) such as phenolic compounds can overlap with these peaks (Reynolds, 2003; Yamashita and Tanoue, 2003b; Maie et al., 2005). As such, protein-like fluorescence data presented in Table 2 must be interpreted with these issues in mind.

Additional information on proteinaceous materials can be obtained from the peak position of Peak T. This peak is known to shift depending on the molecular environments surrounding the Trp moiety. A blue-shift occurs when the Trp moiety is shielded from the surrounding water or hydrogen bonding groups (Lakowicz, 1999). As such,

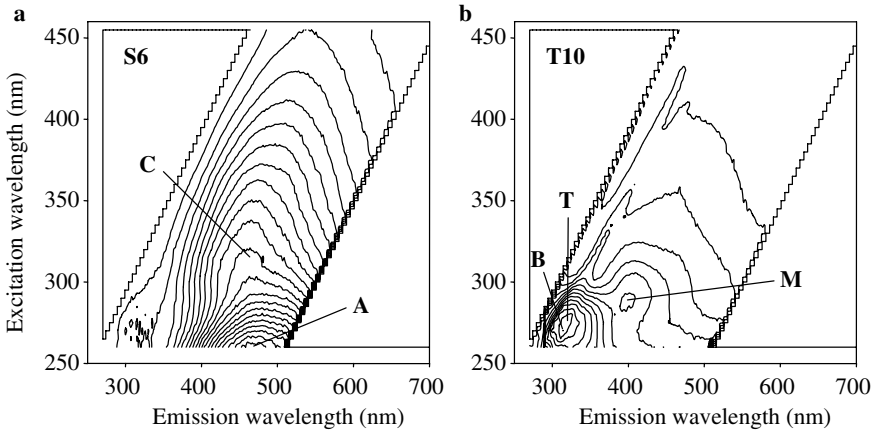

Fig. 2. Examples of EEM spectra of UDOM samples collected from the FCE; (a), S6; (b), T10. Peak A, UV humic-like; Peak C, visible humic-like; peak B, Tyr-like; peak T, Trp-like; peak M, marine humic-like. Peak assignment is according to Coble et al. (1998). See also Table 2.

Table 2
Peak assignment for the EEM spectra of FCE-UDOM samples according to Coble et al. (1998). Peak positions, maximum peak intensity, and peak ratios were described

Sample site	A (UV humic-like)		C (Visible humic-like)		M (Visible marine humic-like)		B (Tyr-like, protein-like)		T (Trp-like, protein-like)		A:C
	Ex/Em	F_{max}[a]	Ex/Em	F_{max}[a]	Ex/Em	F_{max}[a]	Ex/Em	F_{max}[b]	Ex/Em	F_{max}[a]	
T2	⩽260/460	7.3	320–360/420–460	2.8 ± 0.5	I	I	275/304	0.7	275/335	I	2.6
T7	⩽260/468	4.8	320–360/420–460	1.9 ± 0.5	I	I	275/302	0.5	275/319	0.8	2.5
T10	⩽260/468	0.8	320–360/420–460	0.34 ± 0.08	290/396	0.9	275/302	1.6	275/325	1.8	2.4
									275/312	1.8	
S4	⩽260/464	8.1	320–360/420–460	2.8 ± 0.5	I	I	275/307	0.7	275/319	0.6	2.9
									275/325	0.6	
									275/342	0.7	
S6	⩽260/464	6.5	320–360/420–460	2.5 ± 0.5	I	I	275/302	0.5	275/319	0.6	2.6
									275/335	0.6	
Coble[b]	⩽260/400–460		320–360/420–460		290–310/370–410		275/305		275/340		

I, indeterminable. The M peak was less intense compared to the much more intense C peak that strongly interferes in this region. ND, not detected.
[a] Peak fluorescence intensity in quinine sulfate equivalents (QSU) divided by [DOC] ($mg\,L^{-1}$).
[b] Coble et al. (1998).

shorter emission wavelength of peak T for FB–UDOM (Ex = 325 nm) compared to free-Trp (340 nm) may suggest that Trp is folded/shielded or occluded/encapsulated in a relatively hydrophobic molecular environment, and thereby protected from enzymatic degradation. Abiotic complexation of proteinaceous materials with DOM has been suggested to reduce biodegradation rates of DON (Keil and Kirchman, 1994). This might be one of the reasons for the low bioavailability of DON (Keil and Kirchman, 1994; Hedges et al., 2000b).

3.1.3. C:N atomic ratios

The C:N ratio is regularly used to assess the source of NOM and supplement interpretation of stable isotope data. The highest C:N ratios of FCE–UDOM samples were observed for the SRS mangrove sites (~28) and the lowest for FB (~16) (Table 3). These values were within the range of reported values for other freshwater and marine UDOM (Table 3).

3.1.4. Stable C isotope ratios

The $\delta^{13}C$ value has been most widely used to assess the source and biogeochemical cycling of NOM (Lajtha and Michener, 1994). The $\delta^{13}C$ values for TS and SRS UDOM samples were indicative of terrestrial C3 type higher plant inputs with an average (±SD) $\delta^{13}C$ value of $-26.7 \pm 1.1‰$ (Table 3). In contrast, $\delta^{13}C$ of the FB sample is considerably heavier ($\delta^{13}C = -14.4‰$) and fall between that of marine plankton ($-18‰$ to $-24‰$) and the seagrass, *Thalassia testudinum* ($-5.2‰$ to $-13.5‰$) (Table 3). The mangrove sites, (S4, S6, and T7) UDOM had the most depleted $\delta^{13}C$ values (~$-27‰$), consistent with the signature for mangrove leaves (Table 3). Site T2, which is located in a sawgrass prairie with abundant periphyton assemblages, was comparatively enriched in $\delta^{13}C$ (~$-25‰$). Periphyton is a matrix of phytoplankton, algae, and other microbes, and its $\delta^{13}C$ values in the Northern Everglades were found to range from -20 to $-32‰$ (Kendall et al., 2001). The ^{13}C isotopic signature of UDOM has been shown to be similar to the total DOC pool (Benner et al., 1997), and Table 3 shows that $\delta^{13}C$ values of UDOM also appear to reflect source signatures. Thus, the enriched $\delta^{13}C$ value for site T2 may be attributed to an abundance of periphyton, a dominant feature of sloughs in the Everglades (Inglett et al., 2004).

3.1.5. Stable N isotope ratios

The $\delta^{15}N$ values reflect the source and biogeochemical processing of N, and thus can provide useful insight into N cycling and ecosystem functioning (Lajtha and Michener, 1994). The $\delta^{15}N$ values of UDOM samples were fairly consistent throughout the sample set with an average (±SD) $\delta^{15}N$ value of $3.4 \pm 0.1‰$ (Table 3). The $\delta^{15}N$ values of UDOM in the Everglades were close to those of soils and periphyton assemblages in freshwater marsh sites (~$3‰$) while higher than those for sawgrass (~$0‰$) (Childers and Wozniak, pers. comm.). Considering that phytoplankton and other microorganisms contain large amounts of N-containing compounds (Table 3), a closer resemblance of $\delta^{15}N$ values between UDOM and periphyton might suggest that periphyton assemblages are an important source of UDON. The $\delta^{15}N$ value of the UDOM at FB (T10) fell into the range of those for seagrass, *Thalassia testudinum*, at the corresponding site (from $2‰$ to $4‰$; Fourqurean et al., 2005). The $\delta^{15}N$ value of seagrass blades vary seasonally and spatially (Fourqurean et al., 2005), and the variation might influence the $\delta^{15}N$ values of UDOM in FB. We could not assign a specific source of UDON in FB, i.e., allochthonous (produced in FB) vs. autochthonous (derived from the Everglades), from the N stable isotope ratio, because the seasonal and spatial variation in the $\delta^{15}N$ values was larger than the variation among vegetation types.

3.1.6. Characteristics of UDOM in different zones

Optical properties of UDOM at the freshwater marsh site T2 showed intermediate values between those of mangrove marshes and FB (Table 1). This was attributed to the site's dual microbial (periphyton) and terrestrial (sawgrass) character, and was corroborated by the $\delta^{13}C$ value. UDOM at mangrove sites (S4, S6, and T7) was more enriched in aromatic-C and had the most terrestrial characteristics with the highest $SUVA_{254}$ and longest λ_{max} values (McKnight et al., 2001). The $\delta^{13}C$ values of UDOM at mangrove sites were identical with that of mangrove biomass (Table 3). As such, mangroves are considered to be a significant contributor to the UDOM at these locations, as corroborated by previous findings (Maie et al., 2005, 2006a,b). Optical properties of FB-UDOM (T10; low $SUVA_{254}$, high S, shorter λ_{max}, and high FI values) suggested that this UDOM (T10) had the highest microbial signature among the all studied sites. The S value for FB was lower than those of typical oligotrophic blue waters (0.025) (Blough and Vecchio, 2002), which probably reflects some contribution of terrestrial- and/or seagrass community-derived DOM. This interpretation is also supported by a unique EEM spectrum, low C:N ratio, and the remarkably enriched $\delta^{13}C$ value of FB–UDOM (~$-14.4‰$). From the $\delta^{13}C$ values of suspended particles that are assumed to be composed of mainly phytoplankton ($-18‰$ to $-22‰$; Evans and Anderson, personal communication) and the dominant seagrass species in FB (*T. testudinum*, -7 to $-9‰$; Fourqurean et al., 2005), it was estimated that seagrass contributed 30–60% of the UDOM at T10. This may be a conservative estimation since the influence of terrestrial-derived DOM was ignored in this calculation. However, DOM derived from the Everglades is not considered to be a major source of DOM at T10, since the loading of freshwater from the Everglades is low and optical and chemical properties of DOM are very different between the two (Maie et al., 2005, 2006a).

Photobleaching is important in the processing of DOM in aquatic environments (Vodacek et al., 1997; Kowalczuk et al., 2003), and this may be particularly impotant in FB, a

Table 3
Summary table of C:N atomic ratios, stable isotope compositions of C and N, % C and N contributions to total hydrolysable amino acids in UDOM from different locations

Sample type	$[C:N]_a$	$\delta^{15}N$	$\delta^{13}C$	% AA-N	%AA-C	References
UDOM samples from this study (water source/main vegetation/sediment type)						
T2 (freshwater/sawgrass-periphyton/calcareous)	26.0	3.40	−25.0	24	3.4	This study
T7 (micro-tidal/dwarf mangrove-periphyton/calcareous)	22.0	3.46	−26.9	28	4.5	This study
T10 (micro-tidal/seagrass/calcareous)	15.8	3.25	−14.4	34	7.8	This study
S4 (tidal/dwarf mangrove/peat)	27.8	3.50	−27.5	22	2.9	This study
S6 (tidal/tall mangrove/peat)	28.0	3.38	−27.2	28	3.5	This study
Literature/Reference Values						
UDOM						
Surface ocean						
Sargasso Sea and Gulf of Mexico	~17			29/17	~4–6	McCarthy et al. (1996)
Pacific and Atlantic Oceans	~15–17	7 to 8	−22 to −21			Benner et al., 1997
Gulf of Mexico	18	9.5				Benner et al. (1997)
Arctic Ocean			−23 to −22			Opsahl et al. (1999)
Marine			−23 to −20			Wang et al. (2004)
Fresh water/coastal						
Fresh and coastal			−31 to −24			Wang et al. (2004)
Delaware Estuary (USA) 1–30 kDa	17–30		−26 to −22	7–26	1.5–4.2	Mannino and Harvey (2000a,b)
Amazon River	27–52		−30 to −28	13.5 ± 1.7	1.0–1.9	Hedges et al. (1994)
Mississippi River	13–29					Benner and Opsahl (2001)
DOM						
Bulk DOM from bay to ocean transect in NW Pacific					0.9–6.9	Yamashita and Tanoue (2003a)
Fresh algal-derived DOM from Arctic ice floe					7.4	Amon et al. (2001)
Oceanic systems (Surface water)	13.6 ± 2.8		−23.6 to −19.6			Bronk (2002); Bauer (2002)
Coastal/continental shelf	17.7 ± 4.3					Bronk (2002)
Estuarine	21.1 ± 14.3					Bronk (2002)
Selected Rivers	25.7 ± 12.5					Bronk (2002)
Possible source materials						
C3 plants			−35 to −25			Fry (1991)
C4 plants			−14 to −10			Fry (1991); Deines (1980)
Aquatic algae		−4 to +3	−34 to −18			Fry (1991)
Higher plants		−9 to +2				Fry (1991)
Vascular plants (tundra ecosystem)		−1.6 to +6				Nadelhoffer et al. (1996)
Terrestrial sources			−28 to −23			Harvey and Mannino (2001)
Vascular plants	>50			23–79	0.35–17	Cowie and Hedges (1992)
Macrophytes				45–50	28	Cowie and Hedges (1992)
Zooplankton				39–66	65–100	Cowie and Hedges (1992)
Fungi				50	50	Cowie and Hedges (1992)
Ancient sediments				~10%		Cowie and Hedges (1992)
Bacteria	3.7 ± 0.2					Lee and Fuhrman (1987)
Bacteria				82–100	50–56	Cowie and Hedges (1992)
Phytoplankton				40–80	50–100	Cowie and Hedges (1992)
Phytoplankton	6.6					Lee and Fuhrman (1987)
Mangrove leaves						
South Florida			−29 to −25			Lin and Sternberg (1992)
Florida (drawf mangroves)		−5				Fry et al. (2000)
Florida (tall mangroves)		−3				Fry et al. (2000)
Key Largo, tall, Florida		7				Fry et al. (2000)
Biscayne Bay, young/canal, Florida		12				Fry et al. (2000)

Mangroves, Australia		−32.2 to −24.6	Andrews et al. (1984)
Dwarf, *R. mangle* leaves, Belize	−10 (mean)	−25 (mean)	Wooller et al. (2003)
Tall, *R. mangle* leaves, Belize	0 (mean)	−28 (mean)	Wooller et al. (2003)
Periphyton & macrophytes			
Periphyton	−1 to 6.5	−32 to −20	Kendall et al. (2001)
Adjacent to canal	+4 to 12		Childers and Jaffé (2004)
4 km from canal	−1 to 5		Childers and Jaffé (2004)
Everglades Water Conservation Area 2A, Florida (canel to marsh)	0 to +5	−30 to −26	Kendall et al. (2001)
Seagrass			
W. Florida Bay, primarily *Thalassia*	−1 to −4		Corbette et al. (1999)
NE Florida Bay, primarily *Thalassia*	+6 to 13		Corbette et al. (1999)
S. Florida, *Thalassia*	+0.7 to 3.3	−9.6 to −7.2	Anderson and Fourqurean (2001)
S. Florida, *Thalassia*	+1.1 to 2.2	−10.4 to −7.2	Anderson and Fourqurean (2003)
S. Florida, *Thalassia*	−4.3 to +9.4	−13.5 to −5.2	Fourqurean et al. (2005)
Average for *Thallassia*, *Zostera*, and *Halodule*		~−10	Fry and Sherr (1984)
Apalachicola Bay, Florida			
Sawgrass (*Cladium jamaicense*)		−26.1	Chanton and Lewis (2002)
Sawgrass (*C. jamaicense*), dead		−24.7	Chanton and Lewis (2002)
Cattail (*Typha* sp.)		−27	Chanton and Lewis, 2002

shallow, subtropical ecosystem (Scully et al., 2004; Maie et al., 2005). A large area on the bottom of FB is covered with dense seagrass beds (Zieman et al., 1989), which are expected to contribute a large amount of DOM including phenolic compounds to surrounding waters (Ziegler and Benner, 1999; Maie et al., 2006b). However, the aromaticity of FB-(U)DOM is low (Maie et al., 2005), which may be attributed to its high susceptibility to photodegradation (Scully et al., 2004) and to the LMW characteristics of phenolic compounds leached from seagrass (Maie et al., 2006b). The optical properties of FB are thus consistent with contributions from multiple sources of UDOM as well as UDOM transformations such as photobleaching with possible subsequent microbial transformations.

3.2. Molecular characterization of UDON

3.2.1. ^{15}N CPMAS NMR spectra

^{15}N CPMAS NMR has been used to determine the speciation of organic N in NOM (e.g., Knicker, 2004). While much ^{15}N CPMAS NMR work has been applied to soil, coal, and sediment OM (Knicker et al., 1993, 2000; Knicker and Hatcher, 1997), very little has been done with regards to DON (McCarthy et al., 1997; Aluwihare et al., 2005). To the best of our knowledge this work represents the first application of ^{15}N NMR to characterize freshwater and estuarine UDON.

Based on the ^{15}N CPMAS NMR spectra of our UDOM samples (see Fig. 3), most of the detected N was in the form of amide-N (−240 to −285 ppm; i.e., proteinaceous N). A noticeable signal of pyrrolic-N (−145 to −240 ppm) was detected on the shoulder of the amide-N peak for T2, S4, and S6. Note that the pyrrolic-N signal usually does not show up as a distinct peak unless it becomes dominant, but widens the skirt of the amide peak to a higher magnetic field (Abe et al., 2005; Maie et al., 2006c). A pyridinic-N (−25 to −90 ppm) signal was not detected above the noise level. The dominance of amide-N coincides with other reports on the characterization of N species in NOM in various environments (Knicker et al., 1993; McCarthy et al., 1997; Vairavamurthy and Wang, 2002; Aluwihare et al., 2005). However, the presence of a noticeable intensity of pyrrolic-N signal in some of the FCE samples is surprising since pyrrolic-N has mostly been found in highly aromatic and charred/fossilized OM (Knicker et al., 1993; Knicker and Hatcher, 1997; McCarthy et al., 1997; Knicker et al., 2000; Vairavamurthy and Wang, 2002), and the aromaticity of FCE–UDOM is not particularly high (Maie et al., 2005). Possible sources of pyrrolic-N will be discussed in the following section.

3.2.2. XPS-N1s spectra

XPS-N1s is a complementary technique to ^{15}N CPMAS NMR and is used to identify and quantify N species (Abe and Watanabe, 2004; Abe et al., 2005). For example, although amide-N and pyrrolic-N are not distinguishable in N1s spectra, pyridinic-N is better observed since the

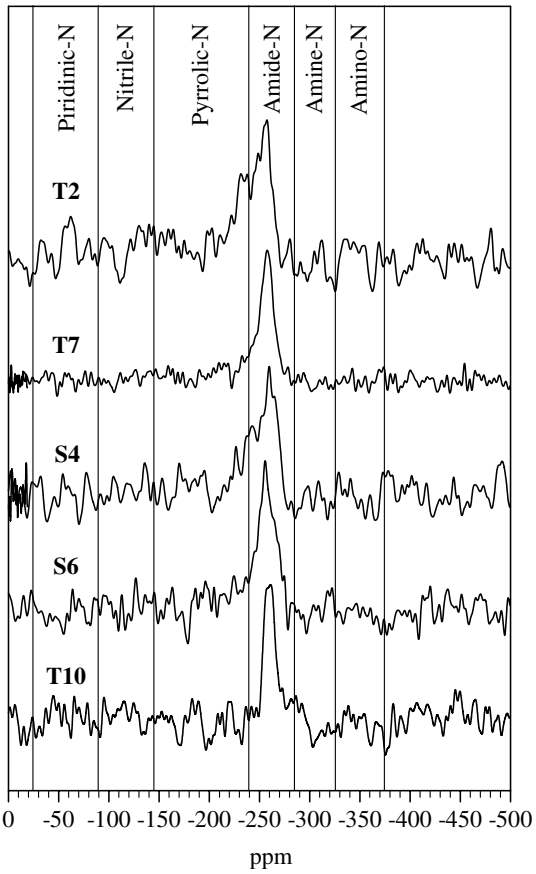

Fig. 3. ^{15}N CPMAS NMR spectra of UDOM samples collected from the FCE.

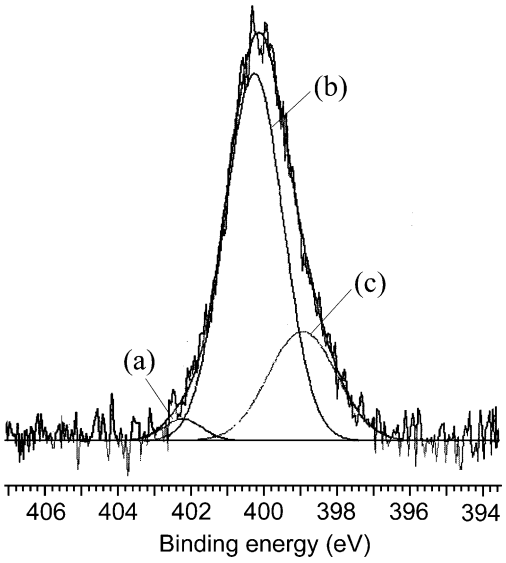

Fig. 4. An example of XPS-N1s spectra of UDOM samples collected from the FCE (T2); (a) primary amine group; (b) peptide bond N group; (c) pyridinic-N group.

Table 4
X-ray photoelectron spectroscopy (XPS)-based N composition of UDOM samples collected from the FCE

Sample site	Pyridinic N 398.8–399.1[a]	Peptide bond N 400.2–400.5	Primary amine N 402.2–402.5
T2	24.7	72.4	2.9
T7	24.3	72.2	3.5
T10	18.5	74.2	7.3
S4	19.8	75.1	5.1
S6	21.1	76.1	2.8

[a] Binding Energy (eV)

signal intensity is the same for all N species (^{15}N CPMAS NMR tends to provide conservative values for non-amide-N). An example of an XPS-N1s spectrum is shown in Fig. 4. The binding energy of N differs depending on the N species, and the spectrum shows the distribution profile. Consistent with the ^{15}N CPMAS NMR results, amide N was the major form of N (74.0 ± 1.7%), followed by pyridinic-N (21.7 ± 2.7%), and primary amine N (4.3 ± 1.9%) (Table 4). This is to our best knowledge the first result of N1s spectra of UDOM samples in aquatic environments. A notable feature of the N1s spectra of the FCE–UDOM samples is the very high abundance of pyridinic-N, especially for T2 and T7 (24.5 ± 0.2%). This value is unexpectedly high in comparison with humic acids (HAs) extracted from various soils (3.0% to 18.7%), where only highly humified HAs contained more than 10% of pyridinic-N (Abe and Watanabe, 2004). This result might seem inconsistent with the ^{15}N CPMAS NMR data where pyridinic-N was not observed above the noise level. In contrast to XPS, however, ^{15}N NMR underestimates pyridinic-N because (1) this N-form does not have an attached proton resulting in a slower cross-polarization, (2) Pyridinic-N has a wide range of chemical shifts so the peak tends to submerge into the noise signal in NMR, and (3) chemical shift anisotropy of pyridinic-N is larger than that of pyrrolic-N (Kelemen et al., 2002). Indeed, Kelemen et al. (2002) also detected 27 mol% of pyridinic-N in kerogen by XPS-N1s while it was not detected above the noise level on their ^{15}N CPMAS NMR spectrum.

While the pyridinic-N concentration in HAs detected by XPS has been shown to have a positive correlation with ^{13}C NMR-based aromatic-C concentration (Abe et al., 2005), the high concentration of pyridinic-N in the FCE–UDON is surprising because the aromatic-C concentration of FCE–UDOM is relatively low (Maie et al., 2005). However, only a limited number of UDOM samples have been analyzed so far regarding N speciation (McCarthy et al., 1997; Aluwihare et al., 2005). The sources of this aromatic-N are unclear, but could possibly include soot/charred materials produced by wild fire events, which are a common natural phenomenon during the late dry season in the Everglades. Indeed, high charcoal concentrations have been observed in surface soils of the Everglades (Saunders et al., 2006). Dry and wet deposition are other significant sources of N in FB (Boyer and Keller, 2003), and around 15–30% of wet deposition in coastal region is considered to be DON (Paerl et al., 2001). As such, aerosols that contain soot/charred materials might also contribute to the source of aromatic-N. In addition, Vairavamurthy and

Wang (2002) detected a relatively high concentration (~20%) of pyridinic-N in a sediment collected from FB by using K-edge XANES spectroscopy. The authors inferred that the formation mechanisms of pyrrolic-N and pyridinic-N are different, and proposed a possible mechanism for the formation of pyridinic structures via a reaction between ammonia and reactive carbonyl groups derived from phenolic compound such as protocatechuic acid. Seagrass leaches a large amount of reactive phenolic compounds (Maie et al., 2006b), as well as proteins (Rublee and Roman, 1982). As such, pyridinic-N might be produced *in situ* in sediments and/or water in FB, and possibly elsewhere in the FCE. The exact source, the mechanism of formation, and reactivity (photochemical and microbial) of this aromatic-N in aquatic environments remain currently unknown.

3.2.3. Total HAA composition

Although, amide-N is the predominant form of N in our UDOM samples as is indicated by ^{15}N NMR and XPS-N1s spectra, not all amide-N is hydrolysable (Knicker and Hatcher, 1997; Knicker, 2004; Abe et al., 2005; Aluwihare et al., 2005). A recent study showed that the hydrolysable amide-N in aquatic environments is mainly composed of two chemically distinct classes of molecules, namely, proteins and *N*-acetyl amino polysaccharides (*N*-AAPs) (Aluwihare et al., 2005). *N*-AAPs are considered to be labile in the long term since surface ocean waters contain higher concentration of *N*-AAPs than the deep ocean (Aluwihare et al., 2005). These authors report that much of the amid-N in deep ocean waters is in fact biologically recalcitrant. However, hydrolysable proteins have been reported to be biolabile, to experience relatively high rates of biodegradation and be important for microbial loop energetics (Amon et al., 2001; Yamashita and Tanoue, 2003a). As such, the concentration and composition of HAAs, which is a measure of hydrolysable proteins in DOM, provides information that is useful in determining its potential to function as a nutritional food source (Cowie and Hedges, 1994). Relatively high percentages of HAA-C (3–8%) and HAA-N (22–34%) were detected in the FCE–UDOM samples (Table 3). Since fresh UDOM exhibits higher %HAA-C and %HAA-N (Harvey and Mannino, 2001; Benner and Kaiser, 2003), the FCE–UDOM is considered to be relatively fresh. An increasing trend in both %HAA-C and %HAA-N was observed along the fresh, to estuarine, to bay waters transect (Table 3), suggesting significant sources of labile UDOM from the mangrove fringe and estuarine environments. The very high %HAA-C and %HAA-N values at T10 may be attributed to the shift from N-poor vascular plant UDON to N-rich marine biomass (phytoplankton and seagrass) derived UDON. Jones et al. (2005) also reported an increasing contribution of microbial-derived (peptidoglycan) HAA in UDON along a salinity gradient in the FCE by examining the D/L ratios of HAAs.

Although the HAA composition is fairly uniform across a wide range of ecosystems, it can vary depending on its diagenetic history as a result of preferential degradation/preservation of specific AAs (Cowie and Hedges, 1992; Dauwe and Middelburg, 1998; Dauwe et al., 1999; Yamashita and Tanoue, 2003a). The HAA composition of the FCE–UDOM was rich in Val, Ile, but poor in Ala compared to the UDOM in other rivers and estuaries (Table 5), which agrees with typical features of fresh DOM (Yamashita and Tanoue, 2003a). Site T10 has a higher Ser (11.7%) and lower Gly (15%) abundance than the other sites (7.2–8.3% and 16.9–23.3%, respectively). This feature was also observed in the very high molecular weight fraction of DOM (VHMWDOM; smaller than 0.2 μm but larger than 30 kDa) in the Delaware estuary (Mannino and Harvey, 2000a) and this high Ser concentration was attributed to phytoplankton-derived OM. Since both free floating and epiphytic algae are considered potentially important sources of DOM in FB, the explanation above may also be feasible in this ecosystem.

Non-protein derived AA distributions do not generally respond to source changes and are used as measures of degradation/diagenesis. In particular, BALA and GABA are good indicators of diagenetic alterations (Cole and Lee, 1986; Cowie and Hedges, 1994), and are thought to be mainly produced through microbial metabolism (Lee and Cronin, 1982), since these AAs are absent or present only in trace amounts in most organisms (Cowie and Hedges, 1992). Our UDOM samples showed relatively low yields of non-protein HAAs (~2–4 mol% BALA + GABA;

Table 5
Amino acid composition (mol%) of UDOM collected from the FCE

Amino acid	T2	T7	T10	S4	S6
Asp (aspartic acid)[a]	13	8.1	12	13	13
Glu (glutamic acid)[b]	8.5	7.6	9.4	9.2	9.8
Ser (serine)	8.3	7.2	11.7	8	7.6
His (histidine)	0.5	0.7	0.4	0.7	0.8
Gly (glycine)	16.9	23.3	15	18.8	17.5
Thr (threonine)	9.3	5.7	11	8	7.6
Arg (arginine)	3	3.1	2.2	2.6	3
BALA (β-alanine)	2.4	3.1	1.8	2.8	2.2
Ala (alanine)	11.7	10.3	14.1	11.7	11.9
Tyr (tyrosine)	1.5	1.2	1.2	1.2	1.4
GABA (γ-aminobutyric acid)	0.8	0.8	0.4	0.8	0.6
AABA (α-aminobutyric acid)	0	0	0	0	0
Met (methionine)	0	0	0	0	0
Val (valine)	6.7	5.7	6.4	6.7	6.8
Phe (phenylalanine)	3.2	3.4	2.3	2.6	2.8
Ileu (isoleucine)	5.5	7.5	5.4	4.8	4.9
Leu (leucine)	5.4	5.1	3.8	4.9	5.2
Orn (ornithine)	0.4	1	0.4	0.4	0.4
Lys (lysine)	2.8	6.2	2.5	3.9	4.4
DI_P (Dauwe et al., 1999)[c]	−0.2	0.6	−0.7	−0.4	−0.2
DI_D (Yamashita and Tanoue 2003a)[d]	6.1	7.5	4.3	4.5	5.2

[a] Aspartic acid + asparagine.
[b] Glutamic acid + glutamine.
[c] Degradation index which was calculated quating the data by Dauwe et al. (1999).
[d] Degradation index which was calculated quating the data by Yamashita and Tanoue (2003a).

Table 5), which again supports the relatively fresh origin of the FCE–UDOM. For comparison, note that while seawater UDOM mol% (BALA + GABA) was found to be ~1–3%, Amazon River lower tributaries UDOM was ~7% (Cowie and Hedges, 1994; Hedges et al., 1994; McCarthy et al., 1996). Orn and AABA concentrations in our UDOM samples were less than 1% and below the detection limit, respectively. Orn is an intermediate product in the metabolism of Arg (Garrett and Grisham, 2005) but the amount of Orn produced through this pathway is also thought to be minor because like BALA and GABA, it is absent or present only in trace amounts in higher organisms (Cowie and Hedges, 1992). The non-protein AA, AABA, is a diagenetic product formed upon dehydration of Thr. This non-protein AA has been found in sediments but not in our FCE–UDOM samples or in most UDOM samples reported in the literature (McCarthy et al., 1996).

The degradation index (DI; Dauwe et al., 1999), which is a proxy for the diagenetic state of the UDON based on the HAA compositions, is shown in Table 5. Note that DI_D was calculated using reference datasets for DOM (Yamashita and Tanoue, 2003a), and DI_P for POM (Dauwe et al., 1999). For comparative purposes, the $DI_{D,P}$ was also calculated for POM and UDOM from other river/estuarine systems based on published literature data (Table 6) (Hedges et al., 1994; Mannino and Harvey, 2000a). While the DI_P value was consistently lower than the DI_D value of the same sample (Table 6), a significant positive correlation was observed between the two ($r^2 = 0.86$). A higher $DI_{D,P}$ value (lower diagenetic state) was observed for a larger size fraction collected from the same site (i.e., POM > VHMWDOM > UDOM), which agrees with the size-reactivity continuum hypothesis (Hedges et al., 1994, 2000a; Amon and Benner, 1996; Mannino and Harvey, 2000a). When comparing DI values among UDOM in different environments, FCE–UDOM and Amazon River upper tributaries UDOM were significantly higher than Amazon River lower tributary UDOM and the Delaware Estuary UDOM. Note that the DI of the Delaware Estuary UDOM was somewhat underestimated due to exclusion of the VHMWDOM fraction with a high DI value (4.3 ± 1.3). The influence of the VHMWDOM fraction will be, however, minor since the concentrations of HAA in the VHMWDOM is about one-eighth of that of UDOM (Mannino and Harvey, 2000a). On the other hand, HAA concentrations of FCE–UDOM (11.1 ± 5.2 mg gUDOC^{-1}) were significantly higher than for the Amazon River upper and lower tributaries (4.5 ± 0.8 and 3.6 ± 0.6, respectively) (Hedges et al., 1994, 2000a). As such, the major reasons for the low degree of degradation of FCE–DOM may be attributed to both the low microbial activity and the high DON productivity.

4. Summary

Coastal zones are highly productive environments, where nutrient cycling is a key ecological driver (Capone, 2000). DON often represents a major portion of the total N in coastal/estuarine ecosystems, particularly in oligotrophic systems such as the Everglades, and is considered to play an important role in fueling the microbial loop and controlling primary and secondary productivity (Bronk, 2002). Therefore, characterizing DON at the molecular level, determining its bioavailability, and photodegradability, and its involvement in diverse biogeochemical processes is crucial for a better understanding of the importance of DON in biogeochemical cycles of aquatic environments. In this study, the DON (and UDON) from the highly oligotrophic FCE was characterized, and suggested that although oligotrophic, this ecosystem contains primarily relatively fresh, autochtonous DON (based on HAA data), which can be of dual higher plant and periphyton/planktonic origin (based on stable isotope and fluorescence data). Although amide-N was the major form of UDON determined (based on ^{15}N NMR and XPS-N1s data), and in agreement with other reports (McCarthy et al., 1997; Aluwihare et al., 2005), this DON seems resistant to biodegradation. In fact, aromatic (pyridinic and pyrrolic) N was also present at relatively high concentrations (based on ^{15}N NMR and XPS-N1s data), which could be one factor in reducing its overall lability. In addition to the high aromatic nature of this DON, this study

Table 6
Comparison of degradation index (DI) between different size fractions and different environments

Location	Sample type	Number of samples	DI (±SD) Dauwe et al. (1999)	DI (±SD) Yamashita and Tanoue (2003a)
Florida coastal everglades	UDOM (<0.7 μm, >1 kDa)	5	−0.17 ± 0.47 C	5.50 ± 1.32 C
Amazon River Upper Tributaries[a]	POM (>0.1 μm)	12	0.33 ± 0.40 B	8.81 ± 1.49 B
	UDOM (<0.1 μm, >1 kDa)	6	−0.10 ± 0.17 C	5.75 ± 0.74 C
Amazon River Lower Tributaries[a,b]	POM (>0.1 μm[a] or >0.5 μm[b])	17	0.85 ± 0.18 A	9.62 ± 0.90 B
	UDOM (<0.1 μm[a] or <0.5 μm[b], >1 kDa)	11	−0.66 ± 0.20 D	2.16 ± 0.97 D
Delaware Estuary[c]	POM (<3 μm, >0.2 μm)	7	1.00 ± 0.48 A	12.60 ± 2.11 A
	VHDOM (<0.2 μm, >30 kDa)	6	−0.90 ± 0.30 D	4.31 ± 1.33 C
	DOM (<30 kDa, >1 kDa)	7	−1.38 ± 0.18 E	−0.76 ± 1.32 E

[a] Hedges et al. (2000a).
[b] Hedges et al. (1994).
[c] Mannino and Harvey (2000a). Different alphabetic letters on the left of the DI refer to significant differences of the DI values on Student's t test at $P < 0.05$.

determined that proteinaceous materials were located in more hydrophobic molecular environments (based on EEM data), and as such might be more resistant to enzymatic degradation (Derenne et al., 1993; Keil and Kirchman, 1994; Knicker, 2004; Knicker and Hatcher, 1997). These observations were made possible thanks to the combined application of a series of complementary advanced analytical techniques.

Overall, the biogeochemistry of DON remains largely unknown in part due to the lack of simple and accessible analytical techniques (Hedges et al., 2000b). This study demonstrates the utility of a multi-methods technique and multi-proxy approach to advance our understanding of DON biogeochemistry. The application of EEM, ^{15}N CPMAS NMR, XPS, and other analytical tools in combination with interdisciplinary biogeosciences investigations represent a potentially rewarding approach in determining the environmental dynamics and ecological importance of DON, the least well understand component of the N-cycle.

Acknowledgments

This study was funded by the National Oceanographic and Atmospheric Administration (COP R.J.) and the National Science Foundation as part of the FCE-LTER program (DEB-9910514). The authors thank the SERC Stable Isotope Laboratory (NSF 9512385) and the SERC Water Quality Laboratory for analytical assistance and the SERC Field Operations Center for logistical support. We acknowledge the constructive comments from two anonymous reviewers, whose input improved the quality of this manuscript. SERC contribution No 328

Associate editor: Jay A. Brandes

References

Abe, T., Maie, N., Watanabe, A., 2005. Investigation of humic acid N with X-ray photoelectron spectroscopy: effect of acid hydrolysis and comparison with ^{15}N cross polarization/magic angle spinning nuclear magnetic resonance spectroscopy. *Org. Geochem.* **36**, 1490–1497.

Abe, T., Watanabe, A., 2004. X-ray photoelectron spectroscopy or nitrogen functional groups in soil humic acids. *Soil Sci.* **169**, 35–43.

Aitkenhead-Peterson, J.A., McDowell, W.H., Neff, J.C., 2003. Sources, production, and regulation of allochthonous dissolved organic matter inputs to surface waters. In: Findlay, S.E.G., Sinsabaugh, R.L. (Eds.), *Aquatic Ecosystems: Interactivity of Dissolved Organic Matter*. Elsevier, Amsterdam, pp. 25–70.

Aluwihare, L.I., Repeta, D.J., Pantoja, S., Johnson, C.G., 2005. Two chemically distinct pools of organic nitrogen accumulate in the ocean. *Science* **308**, 1007–1010.

Amon, R.M.W., Benner, R., 1994. Rapid cycling of high-molecular-weight dissolved organic matter in the ocean. *Nature* **369**, 549–552.

Amon, R.M.W., Benner, R., 1996. Bacterial utilization of different size classes of dissolved organic matter. *Limnol. Oceanogr.* **41**, 41–51.

Amon, R.M.W., Fitznar, H.-P., Benner, R., 2001. Linkages among the bioreactivity, chemical composition, and diagenetic state of marine dissolved organic matter. *Limnol. Oceanogr.* **46**, 287–297.

Anderson, W.T., Fourqurean, J.W., 2001. Spatial and temporal patterns of $d^{13}C$ and $d^{15}N$ from seagrass in South Florida. In: Eleventh Annual V.M. Goldschmidt Conference.

Anderson, W.T., Fourqurean, J.W., 2003. Intra- and interannual variability in seagrass carbon and nitrogen stable isotopes from south Florida, a preliminary study. *Org. Geochem.* **34**, 185–194.

Andrews, T.J., Clough, B.F., Muller, G.J., 1984. Photosynthetic gas exchange and carbon isotope ratios of some mangroves in North Queensland. In: Teas, H.J. (Ed.), *Physiology and Management of Mangroves*, vol. 9, pp. 15–23.

Battin, T.J., 1998. Dissolved organic matter and its optical properties in a blackwater tributary of the upper Orinoco river, Venezuela. *Org. Geochem.* **28**, 561–569.

Bauer, J.E., 2002. Carbon isotopic composition of DOM. In: Hansell, D.A., Carlson, C.A. (Eds.), *Biochemistry of Marine Dissolved Organic Matter*. Academic Press, pp. 405–453.

Benner, R., Biddanda, B., Black, B., McCarthy, M., 1997. Abundance, size distribution, and stable carbon and nitrogen isotopic compositions of marine organic matter isolated by tangential-flow ultrafiltration. *Mar. Chem.* **57**, 243–263.

Benner, R., Kaiser, K., 2003. Abundance of amino sugars and peptidoglycan in marine particulate and dissolved organic matter. *Limnol. Oceanogr.* **48**, 118–128.

Benner, R., Opsahl, S., 2001. Molecular indicators of the sources and transformations of dissolved organic matter in the Mississippi River plume. *Org. Geochem.* **32**, 597–611.

Benner, R., Pakulski, J.D., McCarthy, M., Hedges, J.I., Hatcher, P.G., 1992. Bulk chemical characteristics of dissolved organic matter in the ocean. *Science* **255**, 1561–1564.

Benner, R., Peele, E.R., Hodson, R.E., 1986. Microbial utilization of dissolved organic matter from leaves of the Red Mangrove, *Rhizophora mangle*, in the Fresh Creek Estuary, Bahamas. *Estuar. Coast. Shelf Sci.* **23**, 607–619.

Berg, G.M., Repeta, D.J., LaRoche, J., 2003. The role of the picoeukaryote *Aureococcus anophagefferens* in cycling of marine high-molecular weight dissolved organic nitrogen. *Limnol. Oceanogr.* **48**, 1825–1830.

Blough, N.V., Green, S.A., 1995. Spectroscopic characterization and remote sensing of nonliving organic matter. In: Zepp, R.G., Sonntag, C. (Eds.), *Role of Nonliving Organic Matter in the Earth's Carbon Cycle*. John Wiley, New York, pp. 23–45.

Blough, N.V., Vecchio, R.D., 2002. Chromophoric DOM in the coastal environment. In: Hansell, D.A., Carlson, C.A. (Eds.), *Biogeochemistry of Marine Dissolved Organic Matter*. Academic Press, New York, pp. 509–546.

Boyer, J.N., Fourqurean, J.W., Jones, R.D., 1997. Spatial characterization of water quality in Florida Bay and Whitewater Bay by multivariate analyses: zones of similar influence. *Estuaries* **20**, 743–758.

Boyer, J.N., Keller, B., 2003. Florida Bay science program: a synthesis of research on Florida Bay. In: Nuttle, W. (Ed.), Nutrient dynamics, vol. 5, pp. 1–42.

L. Brand, Nutrient bioassays and the Redfield ratio in Florida Bay. In: Florida Bay and Adjacent Marine Systems Science Conference, 1999, pp. 78–79.

Bronk, D.A., 2002. Dynamics of DON. In: Hansell, D.A., Carlson, C.A. (Eds.), *Biogeochemistry of Marine Dissolved Organic Matter*. Academic Press, New York, pp. 153–247.

Bronk, D.A., Gilbert, P.M., 1993. Application of a ^{15}N tracer method to the study of dissolved organic nitrogen uptake during spring and summer in Chesapeake Bay. *Mar. Biol.* **115**, 501–508.

Bushaw, K.L., Zepp, R.G., Tarr, M.A., Schulz-Jander, D., Bourbonniere, R.A., Hodson, R., Miller, W.L., Bronk, D.A., Moran, M.A., 1996. Photochemical release of biologically labile nitrogen from dissolved organic matter. *Nature* **381**, 404–407.

Capone, D.G., 2000. The marine nitrogen cycle. In: Kirchman, D.L. (Ed.), *Microbial Ecology of the Oceans*. Wiley, New York, pp. 455–494.

Carlsson, P., Graneli, E., 1993. Availability of Humic Bound Nitrogen for Coastal Phytoplankton. *Estuar. Coast. Shelf Sci.* **36**, 433–447.

Chanton, J., Lewis, F.G., 2002. Examination of coupling between primary and secondary production in a river-dominated estuary: Apalachicola Bay, Florida, USA. *Limnol. Oceanogr.* **47**, 683–697.

Childers, D.L., Boyer, J.N., Davis, S.E., Madden, C.J., Rudnick, D.T., Sklar, F.H., 2006. Relating precipitation and water management to nutrient concentrations in the oligotrophic "upside-down" estuaries of the Florida Everglades. *Limnol. Oceanogr.* **51**, 602–616.

Childers, D.L., Jaffé, R., 2004. The southern Everglades integrated monitoring and science work plan, year 3 semi-annual report by the Southeast Environmental Research Center, Florida International University, Miami, Florida; Report for the South Florida Water Management District, West Palm Beach, Florida, USA, 27p.

Cloern, J.E., 2001. Our evolving conceptual model of the coastal eutrophication problem. *Mar. Ecol. Prog. Ser.* **210**, 223–253.

Coble, P.G., 1996. Characterization of marine and terrestrial DOM in seawater using excitation-emission matrix spectroscopy. *Mar. Chem.* **51**, 325–346.

Coble, P.G., Del Castillo, C.E., Avril, B., 1998. Distribution and optical properties of CDOM in the Arabian Sea during the 1995 Southwest Monsoon. *Deep-Sea Res. II* **45**, 2195–2223.

Coble, P.G., Schultz, C.A., Mopper, K., 1993. Fluorescence contouring analysis of DOC intercalibration experiment samples: a comparison of techniques. *Mar. Chem.* **41**, 173–178.

Cole, J.J., Lee, C., 1986. Rapid microbial metabolism of non-protein amino acids in the sea. *Biogeochemistry* **2**, 299–312.

Cook, R.L., Langford, C.H., Yamdagni, R., Preston, C.M., 1996. A modified cross-polarization magic angle spinning ^{13}C NMR procedure for the study of humic materials. *Anal. Chem.* **68**, 3979–3986.

Corbette, D.R., Chanton, J., Burnett, W., Dillon, K., Rutkowski, C., Fourqurean, J.W., 1999. Patterns of groundwater discharge into Florida Bay. *Limnol. Oceanogr.* **44** (4), 1045–1055.

Cory, R.M., 2006. Redox and photochemical reactivity of dissolved organic matter in surface waters. Ph.D. Dissertation, University of Colorado, Boulder.

Cowie, G.L., Hedges, J.I., 1992. Sources and reactivities of amino acids in a coastal marine environment. *Limnol. Oceanogr.* **37**, 703–724.

Cowie, G.L., Hedges, J.I., 1994. Biochemical indicators of diagenetic alteration in natural organic matter mixtures. *Nature* **369**, 304–307.

Dauwe, B., Middelburg, J.J., 1998. Amino acids and hexosamines as indicators of organic matter degradation state in North Sea sediments. *Limnol. Oceanogr.* **43**, 782–798.

Dauwe, B., Middelburg, J.J., Herman, P.M.J., Heip, C.H.R., 1999. Linking diagenetic alteration of amino acids and bulk organic matter reactivity. *Limnol. Oceanogr.* **44**, 1809–1814.

Davis, I.S.E., Childers, D.L., Day, J.J.W., Rudnick, D.T., Sklar, F.H., 2001. Nutrient dynamics in vegetated and unvegetated areas of a Southern Everglades mangrove creek. *Estuar. Coast. Shelf Sci.* **52**, 753–768.

Davis, S.M., 1994. Phosphorus inputs and vegetation sensitivity in the Everglades. In: Davis, S.M., Ogden, J.C. (Eds.), *Everglades: The Ecosystem and its Restoration*. St. Lucie Press, pp. 357–378.

Deines, P., 1980. The isotopic composition of reduced organic carbon. In: Fritz, P., Fontes, J.C. (Eds.), *Handbook of Environmental Isotope Geochemistry*, Vol. 1. Elsevier, New York, pp. 329–406.

Derenne, S., Largeau, C., Taulelle, F., 1993. Occurrence of non-hydrolysable amides in the macromolecular constituent of *Scenedesmus quadricauda* cell wall as revealed by ^{15}N NMR: origin of *n*-alkylnitriles in pyrolysates of ultralaminae-containing kerogens. *Geochim. Cosmochim. Acta* **57**, 851–857.

Dilling, J., Kaiser, K., 2002. Estimation of the hydrophobic fraction of dissolved organic matter in water samples using UV photometry. *Water Res.* **36**, 5037–5044.

Donard, O.F.X., Lamotte, M., Belin, C., Ewald, M., 1989. High sensitivity fluorescence spectroscopy of Mediterranean waters using a conventional or a pulsed laser excitation source. *Mar. Chem.* **27**, 117–136.

Feuerstein, T.P., Ostrom, P.H., Ostrom, N.E., 1997. Isotopic biogeochemistry of dissolved organic nitrogen: a new technique and application. *Org. Geochem.* **27**, 363–370.

Findlay, S.E.G., Sinsabaugh, R.L., 2003. Aquatic ecosystems: interactivity of dissolved organic matter. In: Thorp, J.H. (Ed.), *Aquatic Ecology Series*. Academic Press, New York, pp. 1–512.

Fourqurean, J.W., Escorcia, S.P., Anderson, W.T., Zieman, J.C., 2005. Spatial and seasonal variability in elemental content, delta C-13, and delta N-15 of *Thalassia testudinum* from South Florida and its implications for ecosystem studies. *Estuaries* **28**, 447–461.

Fourqurean, J.W., Jones, R.D., Zieman, J.C., 1993. Process influencing water column nutrient characteristics and phosphorus limitation of phytoplankton biomass in Florida Bay, FL, USA: inferences from spatial distributions. *Estuar. Coast. Shelf Sci.* **36**, 295–314.

Fry, B., 1991. Stable isotope diagrams of freshwater food webs. *Ecology* **72**, 2293–2297.

Fry, B., Bern, A.L., Ross, M.S., Meeder, J.F., 2000. $\delta^{15}N$ Studies of nitrogen use by the Red Mangrove, *Rhizophora mangle* L. in South Florida. *Estuar. Coast. Shelf Sci.* **50**, 291–296.

Fry, B., Sherr, E.B., 1984. ^{13}C measurements as indicators of carbon flow in marine and freshwater ecosystems. *Contrib. Mar. Sci.* **27**, 13–47.

Garrett, R.H., Grisham, C.M., 2005. *Biogeochemistry*. Thomson Brooks/Cole.

Green, S.A., Blough, N.V., 1994. Optical absorption and fluorescence properties of chromophoric dissolved organic matter in natural waters. *Limnol. Oceanogr.* **39**, 1903–1916.

Harvey, H.R., Mannino, A., 2001. The chemical composition and cycling of particulate and macromolecular dissolved organic matter in temperate estuaries as revealed by molecular organic tracers. *Org. Geochem.* **32**, 527–542.

Hedges, J.I., Cowie, G.L., Richey, J.E., Quay, P.D., Benner, R., Strom, M., Forsberg, B.R., 1994. Origins and processing of organic matter in the Amazon River as indicated by carbohydrates and amino acids. *Limnol. Oceanogr.* **39**, 743–761.

Hedges, J.I., Mayorga, E., Tsamakis, E., McClain, M.E., Aufdenkampe, A., Quay, P., Richey, J.E., Benner, R., Opsahl, S., Black, B., Pimentel, T., Quintanilla, J., Maurice, L., 2000a. Organic matter in Bolivian tributaries of the Amazon River: A comparison to the lower mainstream. *Limnol. Oceanogr.* **45**, 1449–1466.

Hedges, J.I., Eglinton, G., Hatcher, P.G., Kirchman, D.L., Arnosti, C., Derenne, S., Evershed, R.P., Kögel-Knabner, I., de Leeuw, J.W., Littke, R., Michaelis, W., Rullkötter, J., 2000b. The molecularly-uncharacterized component of nonliving organic matter in natural environments. *Org. Geochem.* **31**, 945–958.

Inglett, P.W., Reddy, K.R., McCormick, P.V., 2004. Periphyton chemistry and nitrogenase activity in a northern Everglades ecosystem. *Biogeochemistry* **67**, 213–233.

Jaffé, R., Boyer, J.N., Lu, X., Maie, N., Yang, C., Scully, N.M., Mock, S., 2004. Source characterization of dissolved organic matter in a subtropical mangrove-dominated estuary by fluorescence analysis. *Mar. Chem.* **84**, 195–210.

Jones, V., Collins, M.J., Penkman, K.E.H., Jaffé, R., Wolff, G.A., 2005. An assessment of the microbial contribution to aquatic dissolved organic nitrogen using amino acid enantiomeric ratios. *Org. Geochem.* **36**, 1099–1107.

Kaiser, K., Benner, R., 2005. Hydrolysis-induced racemization of amino acids. *Limnol. Oceanogr. Methods.* **3**, 318–325.

Keil, R.G., Kirchman, D.L., 1991. Dissolved combined amino acids in marine waters as determined by a vapor-phase hydrolysis method. *Mar. Chem.* **33**, 243–259.

Keil, R.G., Kirchman, D.L., 1994. Abiotic transformation of labile protein to refractory protein in sea water. *Mar. Chem.* **45**, 187–196.

Kelemen, S.R., Afeworki, M., Gorbaty, M.L., Kwiatek, P.J., Solum, M.S., Hu, J.Z., Pugmire, R.J., 2002. XPS and ^{15}N NMR study of nitrogen forms in carbonaceous solids. *Energy Fuel.* **16**, 1507–1515.

Kendall, C., Silva, S.R., Kelly, V.J., 2001. Carbon and nitrogen isotopic compositions of particulate organic matter in four large river systems across the United States. *Hydrol. Process.* **15**, 1301–1346.

Knicker, H., 2004. Stabilization of N-compounds in soil and organic-matter-rich sediments—what is the difference? *Mar. Chem.* **92**, 167–195.

Knicker, H., Frund, R., Ludemann, H.-D., 1993. The chemical nature of nitrogen in native soil organic matter. *Naturwissenschaften* **80**, 219–221.

Knicker, H., Hatcher, P.G., 1997. Survival of protein in an organic-rich sediment: possible protection by encapsulation in organic matter. *Naturwissenschaften* **84**, 231–234.

Knicker, H., Lüdemann, H.-D., 1995. N-15 and C-13 CPMAS NMR studies of N-15 enriched plant material during 600 days of microbial degradation. *Org. Geochem.* **23**, 329–341.

Knicker, H., Schmidt, M.W.I., Kögel-Knabner, I., 2000. Nature of organic nitrogen in fine particle size separates of sandy soils of highly industrialized areas as revealed by NMR spectroscopy. *Soil Biol. Biochem.* **32**, 241–252.

Kowalczuk, P., Cooper, W.J., Whitehead, R.F., Durako, M.J., Sheldon, W., 2003. Characterization of CDOM in an organic-rich river and surrounding coastal ocean in the South Atlantic Bight. *Aquat. Sci.* **65**, 384–401.

Kroer, N., Jørgensen, N.O.G., Coffin, R.B., 1994. Utilization of dissolved nitrogen by heterotrophic bacterioplankton: a comparison of three ecosystems. *Appl. Environ. Microbiol.* **60**, 4116–4123.

Lajtha, K., Michener, R.H., 1994. Stable isotopes in ecology and environmental science. In: Lawton, J.H., Likens, G.E. (Eds.), *Methods in Ecology*. Blackwell Scientific publications, Oxford, p. 316.

Lakowicz, J.R., 1999. *Principles of Fluorescence Spectroscopy*. Kluwer Academic/Plenum Publishers, Dordrecht/New York.

Lavrentyev, P.J., Bootsma, H.A., Johengen, T.H., Cavaletto, J.F., Gardner, W.S., 1998. Microbial plankton response to resource limitation: insights from the community structure and seston stoichiometry in Florida Bay, USA. *Mar. Ecol. Progress Ser.* **165**, 45–57.

Lee, C., Cronin, C., 1982. The vertical flux of particulate organic nitrogen in the sea: decomposition of amino acids in the Peru upwelling area and the equatorial Atlantic. *J. Mar. Res.* **40**, 227–251.

Lee, S., Fuhrman, J.A., 1987. Relationship between biovolume and biomass of naturally derived marine bacterioplankton. *Appl. Environ. Microbiol.* **53**, 1298–1303.

Lin, G., Sternberg, L.d.S.L., 1992. Differences in morphology, carbon isotope ratios, and photosynthesis between scrub and fringe mangroves in Florida, USA. *Aquat. Bot.* **42**, 303–313.

Lorrain, A., Savoye, N., Chauvaud, L., Paulet, Y.-M., Naulet, N., 2003. Decarbonation and preservation method for the analysis of organic C and N contents and stable isotope ratios of low-carbonated suspended particulate material. *Anal. Chim. Acta* **491**, 125–133.

Lu, X.Q., Maie, N., Hanna, J.V., Childers, D.L., Jaffé, R., 2003. Molecular characterization of dissolved organic matter in freshwater wetlands of the Florida Everglades. *Water Res.* **37**, 2599–2606.

Maie, N., Boyer, J.N., Yang, C.-Y., Jaffé, R., 2006a. Spatial, geomorphological, and seasonal variability of CDOM in estuaries of the Florida Coastal Everglades. Hydrobiologia, in press.

Maie, N., Jaffé, R., Miyoshi, T., Childers, D.L., 2006b. Quantitative and qualitative aspects of dissolved organic carbon leached from plants in an oligotrophic wetland. *Biogeochemistry* **78**, 285–314.

Maie, N., Knicker, H., Watanabe, A., Kimura, M., 2006c. Heterocyclic N in the highly humified humic acids extracted from the subsoil of paddy fields and surface ando soils. *Org. Geochem.* **37**, 12–19.

Maie, N., Yang, C.-Y., Miyoshi, T., Parish, K., Jaffé, R., 2005. Chemical characteristics of dissolved organic matter in an oligotrophic subtropical wetland/estuarine ecosystem. *Limnol. Oceanogr.* **50**, 23–35.

Mannino, A., Harvey, H.R., 2000a. Biochemical composition of particles and dissolved organic matter along an estuarine gradient: sources and implications for DOM reactivitiy. *Limnol. Oceanogr.* **45**, 775–788.

Mannino, A., Harvey, H.R., 2000b. Terrigenous dissolved organic matter along an estuarine gradient and its flux to the coastal ocean. *Org. Geochem.* **31**, 1611–1625.

McCarthy, M., Hedges, J., Benner, R., 1996. Major biochemical composition of dissolved high molecular weight organic matter in seawater. *Mar. Chem.* **55**, 281–297.

McCarthy, M., Pratum, T., Hedges, J., Benner, R., 1997. Chemical composition of dissolved organic nitrogen in the ocean. *Nature* **390**, 150–153.

McKnight, D.M., Boyer, E.W., Westerhoff, P.K., Doran, P.T., Kulbe, T., Andersen, D.T., 2001. Spectrofluorometric characterization of dissolved organic matter for indication of precursor organic material and aromaticity. *Limnol. Oceanogr.* **46**, 38–48.

McKnight, D.M., Harnish, R., Wershaw, R.L., Baron, J.S., Schiff, S., 1997. Chemical characteristics of particulate, colloidal, and dissolved organic material in Loch Vale Watershed, Rocky Mountain National Park. *Biogeochemistry* **36**, 99–124.

Nadelhoffer, K., Shaver, G., Fry, B., Giblin, A., Johnson, L., McKane, R., 1996. ^{15}N natural abundances and N use by tundra plants. *Oecologia* **107**, 386–394.

Obernosterer, I., Benner, R., 2004. Composition between biological and photochemical processes in the mineralization of dissolved organic carbon. *Limnol. Oceanogr.* **49**, 117–124.

Opsahl, S., Benner, R., Amon, R.M.W., 1999. Major flux of terrigenous dissolved organic matter through the Arctic Ocean. *Limnol. Oceanogr.* **44**, 2017–2023.

Paerl, H.W., Boynton, W.R., Dennis, R.L., Driscoll, C.T., Greening, H.S., Kremer, J.N., Rabalais, N.N., Seitzinger, S.P., 2001. Atmospheric deposition of nitrogen in coastal waters: Biogeochemical and ecological implications. In: Valigura, R.A., Alexander, R.B., Castro, M.S., Meyers, T.P., Paerl, H.W., Stacey, P.E., Turner, R.E. (Eds.), *Coastal and Estuarine Studies*. American Geophysical Union, pp. 11–52.

Palenik, B., Morel, F.M.M., 1990. Amino acid utilization by marine phytoplankton: a novel mechanism. *Limnol. Oceanogr.* **35**, 260–269.

Peersen, O.B., Wu, X., Kustanovich, I., Smith, S.O., 1993. Variable-amplitude cross-polarization MAS NMR. *J. Magn. Reson. A.* **104**, 334–339.

Phlips, E.J., Badylak, S., 1996. Spatial variability in phytoplankton standing crop and composition in a shallow inner-shelf lagoon, Florida Bay, Florida. *Bull. Mar. Sci.* **58**, 203–216.

Reynolds, D.M., 2003. Rapid and direct determination of tryptophan in water using synchronous fluorescence spectroscopy. *Water Res.* **37**, 3055–3060.

Robblee, M.B., Barber, T.R., Carlsson, P.R., Durako, M.J., Fourqurean, J.W., Muehlstein, L.K., Porter, D., Yarbo, L.A., Zieman, R.T., Zieman, J.C., 1991. Mass mortality of the tropical seagrass *Thalassia testudinum* in Florida Bay (USA). *Mar. Ecol. Prog. Ser.* **71**, 297–299.

Rublee, P.A., Roman, M.R., 1982. Decomposition of turtlegrass (*Thalassia testudinum* Konig) in flowing sea-water tanks and litterbags: compositional changes and comparison with natural particulate matter. *J. Exp. Mar. Biol. Ecol.* **58**, 47–58.

Saunders, C.J., Gao, M., Lynch, J., Jaffé, R., Childers, D.L., 2006. Reconstructing historic sawgrass and wet prairie slough vegetation in Shark Slough, Everglades National Park, using soil profiles of seeds and molecular markers. Hydrobiologia, in press.

Scully, N.M., Maie, N., Dailey, S.K., Boyer, J.N., Jones, R.D., Jaffé, R., 2004. Photochemical and microbial transformation of plant derived dissolved organic matter in Florida Everglades. *Limnol. Oceanogr.* **49**, 1667–1678.

Seitzinger, S.P., Sanders, R.W., 1997. Contribution of dissolved organic nitrogen from rivers to estuarine eutrophication. *Mar. Ecol. Prog. Ser.* **159**, 1–12.

Sierra, M.M.D., Donard, O.F.X., Lamotte, M., 1997. Spectral identification and behaviour of dissolved organic fluorescent material during estuarine mixing processes. *Mar. Chem.* **58**, 51–58.

Sierra, M.M.D., Donard, O.F.X., Lamotte, M., Ewald, C.B.M., 1994. Fluorescence spectroscopy of coastal and marine waters. *Mar. Chem.* **47**, 127–144.

Simon, M., Rosenstock, B., 1992. Carbon and nitrogen sources of planktonic bacteria in Lake Constance studied by the composition and isotope dilution of intracellular amino acids. *Limnol. Oceanogr.* **37**, 1496–1511.

Stedmon, C.A., Markager, S., Bro, R., 2003. Tracing dissolved organic matter in aquatic environments using a new approach to fluorescence spectroscopy. *Mar. Chem.* **82**, 239–254.

Tezuka, Y., 1990. Bacterial regeneration of ammonium and phosphate as affected by the carbon:nitrogen:phosphorus ratio of organic substrates. *Microbial Ecol.* **19**, 227–238.

Thurman, E.M., 1985. *Organic Geochemistry of Natural Waters*. Kluwer Academic Publishers, Dordrecht.

Tomas, C., Bendis, B., Houchin, L., 1998. Florida Bay algal blooms: spatial and temporal variations in primary production. In: Florida Bay Science Conference.

Traina, S.J., Novak, J., Smeck, N.E., 1990. An ultraviolet absorbance method of estimating the percent aromatic carbon content of humic acids. *J. Environ. Qual.* **19**, 151–153.

Vairavamurthy, A., Wang, S., 2002. Organic nitrogen in geomacromolecules: insights on speciation and transformation with K-edge XANES spectroscopy. *Environ. Sci. Technol.* **36**, 3050–3056.

Vodacek, A., Blough, N.V., DeGrandpre, M.D., Peltzer, E.T., Nelson, R.K., 1997. Seasonal variation of CDOM and DOC in the Middle Atlantic Bight: Terrestrial inputs and photooxidation. *Limnol. Oceanogr.* **42**, 674–686.

Wang, X.-C., Altabet, M.A., Callahan, J., Chen, R.F., 2004. Stable carbon and nitrogen isotopic compositions of high molecular weight dissolved organic matter from four U.S. estuaries. *Geochim. Cosmochim. Acta* **68**, 2681–2691.

Wangersky, P.J., 1993. Dissolved organic carbon methods: a critical review. *Mar. Chem.* **41**, 61–74.

Weishaar, J.L., Aiken, G.R., Bergamaschi, B.A., Fram, M.S., Fujii, R., Mopper, K., 2003. Evaluation of specific ultraviolet absorbance as an indicator of the chemical composition and reactivity of dissolved organic carbon. *Environ. Sci. Technol.* **37**, 4702–4708.

Wheeler, P.A., Kirchman, D.L., 1986. Utilization of inorganic and organic nitrogen by bacteria in marine systems. *Limnol. Oceanogr.* **31**, 998–1009.

Wooller, M., Smallwood, B., Scharler, U., Jacobson, M., Fogel, M., 2003. A taphonomic study of [delta]13C and [delta]15N values in *Rhizophora mangle* leaves for a multi-proxy approach to mangrove palaeoecology. *Org. Geochem.* **34**, 1259–1275.

Yamashita, Y., Tanoue, E., 2003a. Distribution and alteration of amino acids in bulk DOM along a transect from bay to oceanic waters. *Mar. Chem.* **82**, 145–160.

Yamashita, Y., Tanoue, E., 2003b. Chemical characterization of protein-like fluorophores in DOM in relation to aromatic amino acids. *Mar. Chem.* **82**, 255–271.

Ziegler, J.C., Benner, R., 1999. Dissolved organic carbon cycling in a subtropical seagrass-dominated lagoon. *Mar. Ecol. Prog. Ser.* **180**, 149–160.

Zieman, J.C., Fourqurean, J.W., Iverson, R.L., 1989. Distribution, abundance and productivity of seagrasses and macroalgae in Florida Bay. *Bull. Mar. Sci.* **44**, 292–311.

Zieman, J.C., Fourqurean, J.W., Frankovich, T.A., 1999. Seagrass die-off in Florida Bay: Long-term trends in abundance and growth of turtle grass, *Thalassia testudinum. Estuaries* **22**, 460–470.